Journal of Mathematical Chemistry Vol. 27, No. 4, 2000

Simulation of electrochemical behavior of partially blocked electrodes under linear potential sweep conditions

R. Baronas [a], F. Ivanauskas [a,b] and A. Survila [c]

[a] *Vilnius University, Naugarduko 24, 2600 Vilnius, Lithuania*
E-mail: Feliksas.Ivanauskas@maf.vu.lt
[b] *Institute of Mathematics and Informatics, Akademijos 4, 2600 Vilnius, Lithuania*
[c] *Institute of Chemistry, A. Gostauto 9, 2600 Vilnius, Lithuania*

Received 28 July 2000

The paper presents nonlinear model which stands for effective digital simulation of electrochemical behavior of partially blocked electrodes under linear potential sweep and cyclic voltammetry conditions. The model is based on a system of diffusion equations, also involving the Nernst diffusion layer. The mass transport is assumed to be regular in the entire diffusion space. The influence of the thickness of the resist layer on the behavior of the partially blocked electrodes is investigated. The agreement between the theoretical results and experimental ones is obtained to be admirable for several model electrodes with different blocking degree.

KEY WORDS: partially blocked electrodes, modelling, diffusion

1. Introduction

Microelectrodes and their ensembles (arrays) have been investigated recently from both theoretical and experimental point of view. A comprehensive review of papers is given in [1]. High diffusion current densities conditioned by radial flows, and low values of ohmic potential drop are most prominent in the case of ultramicroeletrodes, whose characteristic length is less than 20 μm [1,2]. Modern technologies make it possible to manufacture electrodes of very small dimensions (down to 0.2–1 μm of order) [3], by using different materials.

Because of the currents observed at single electrodes are not high (due to a small area of their surface), the microelectrode ensembles with the above properties are advised to be used for various purposes. The range of application of such microelectrodes is very wide, covering viz. electroanalysis and investigations of kinetics of electrochemical reactions [4–6], usage *in vivo* of microsensors modified by enzymes [7], application of microprobes sensitive to various ions (including H^+) in scanning electrochemical microscopy [8], monitoring of zone distribution in electrophoresis, improvement of liquid chromatographic detectors [9], etc.

0259-9791/00/1200-0267$18.00/0

A hexagonal distribution of unit cells containing active/passive disc electrodes has been analyzed in terms of semi-infinite diffusion in [10–12]. To simplify quantitative description, the cell was divided into two coaxial spaces, with different regularities of mass transport. Such approach made possible to apply the Laplace transform and to obtain analytical expressions. Usually these expressions involved a parameter γ [10], which used to have a physical sense, but was, in fact, a fitting parameter. Experimental data obtained with linear potential sweep (LPS) technique followed the theoretical regularities of the model [11]. Though the employed model electrodes had the photoresist layer of the thickness of 1–2 μm, in mathematical model the electrode surface was assumed to be flat.

This approach was improved in [13–15] where the diffusion in limited space (a concept of a pseudo-Nernst diffusion layer) was taken into account. In addition, the division of diffusion space into two parts was made by means of a plane parallel to the electrode surface.

A digital simulation by using the two-dimensional expanding grid method was performed in [5], involving an image of semi-infinite diffusion. This method exhibited higher peak currents as experimental ones, obtained in [11]. A good agreement between simulated and experimental voltammograms furthermore was observed only at sufficiently low/high rates of potential sweep.

Regardless of certain shortcomings of quantitative description, the following limiting cases of electrochemical behavior of microelectrode arrays are rather well formulated: a linear diffusion to active places describes mass transfer within the range of very short times (high frequencies in the case of impedance). Conversely, a linear diffusion to the entire electrode area proceeds when the time period is sufficiently long one (low frequencies) [4,12].

Semi-infinite diffusion image is generally used in theoretical works. According to this, the diffusion front may infinitely shift from the electrode surface to the bulk of solution. However, if the measurement time is not very short, it is indispensable to take into consideration the consequences of natural convection as well (see, e.g., [16]).

The goal of this research is to propose a model allowing us to simulate effectively the electrochemical behavior of partially blocked electrodes under linear potential sweep conditions. The proposed model is based on diffusion equations involving particularly the Nernst diffusion layer. The model also involves a resist layer of the inactive site of the electrode surface. The mass transport is regular in the entire diffusion space. The influence of the thickness of the resist layer is investigated is this paper. Specifically it is shown that the influence of 1 μm thickness of the resist layer can be significant for relatively small active areas of the partially blocked electrodes.

Definite problems arise when solving analytically the differential equations with the complex geometry of the diffusion space and boundary conditions. Consequently, the proposed mathematical model was solved numerically in this paper. The overload of calculation was the main problem in the digital modelling.

2. Mathematical model

Consider a simple redox-electrode reaction

$$\mathrm{O} + n\mathrm{e} \leftrightarrow \mathrm{R} \tag{1}$$

involving only soluble species. The redox process includes a charge transfer and diffusion. It was assumed that mass transport obeys a finite diffusion regime within a Nernst layer from the electrode/electrolyte boundary. Because of the thickness of the Nernst layer may be different for species O and R, let Ω_O and Ω_R be the diffusion space of O and R, respectively. Note that either $\Omega_\mathrm{O} \subseteq \Omega_\mathrm{R}$ or $\Omega_\mathrm{R} \subseteq \Omega_\mathrm{O}$. Let Γ_O (Γ_R, respectively) be the entire surface of the diffusion space Ω_O (Ω_R), and $\Gamma_\mathrm{O}^\mathrm{N}$ ($\Gamma_\mathrm{R}^\mathrm{N}$) denotes the upper surface only (Nernst layer boundary) of that space ($\Gamma_\mathrm{R}^\mathrm{N} \subset \Gamma_\mathrm{R}$, $\Gamma_\mathrm{O}^\mathrm{N} \subset \Gamma_\mathrm{O}$).

The surface of a solid electrode is generally composed of active (uncovered) and inactive (covered) sites. Since the charge transfer occurs in the active region of the electrode only, let Γ_a be the active region of the electrode ($\Gamma_\mathrm{a} \subset \Gamma_\mathrm{O}$, $\Gamma_\mathrm{a} \subset \Gamma_\mathrm{R}$).

The mathematical model of the reaction (1) can be written as a system of differential equations of the diffusion type:

$$\frac{\partial C_\mathrm{R}}{\partial t} = D_\mathrm{R} \Delta C_\mathrm{R}, \tag{2}$$

$$\frac{\partial C_\mathrm{O}}{\partial t} = D_\mathrm{O} \Delta C_\mathrm{O}, \tag{3}$$

where Δ is the Laplace operator, C_R and C_O are the concentrations of the species R and O, respectively, D_R, D_O are the diffusion coefficients, and t is the time elapsed since the beginning of the electrolysis. The initial conditions ($t = 0$) are

$$C_\mathrm{R}|_{\Omega_\mathrm{O}} = C_\mathrm{R}^0, \qquad C_\mathrm{O}|_{\Omega_\mathrm{R}} = C_\mathrm{O}^0, \tag{4}$$

where C_R^0 and C_O^0 are the initial concentration of the species in the container. The boundary conditions ($t > 0$) are

$$C_\mathrm{R}|_{\Gamma_\mathrm{R}^\mathrm{N}} = C_\mathrm{R}^0, \qquad C_\mathrm{O}|_{\Gamma_\mathrm{O}^\mathrm{N}} = C_\mathrm{O}^0, \tag{5}$$

$$\left.\frac{\partial C_\mathrm{R}}{\partial \mathrm{n}}\right|_{\Gamma \setminus (\Gamma_\mathrm{a} \cup \Gamma_\mathrm{R}^\mathrm{N})} = \left.\frac{\partial C_\mathrm{O}}{\partial \mathrm{n}}\right|_{\Gamma \setminus (\Gamma_\mathrm{a} \cup \Gamma_\mathrm{O}^\mathrm{N})} = 0, \tag{6}$$

$$nFD_\mathrm{R}\left.\frac{\partial C_\mathrm{R}}{\partial \mathrm{n}}\right|_{\Gamma_\mathrm{a}} = -nFD_\mathrm{O}\left.\frac{\partial C_\mathrm{O}}{\partial \mathrm{n}}\right|_{\Gamma_\mathrm{a}} = i(t), \tag{7}$$

with

$$i(t)\big|_{\Gamma_\mathrm{a}} = i_0\left(\frac{C_\mathrm{R}}{C_\mathrm{R}^0}\exp\left(-\frac{\alpha nF}{RT}\big(E_\mathrm{eq} - E(t)\big)\right) - \frac{C_\mathrm{O}}{C_\mathrm{O}^0}\exp\left(\frac{(1-\alpha)nF}{RT}\big(E_\mathrm{eq} - E(t)\big)\right)\right), \tag{8}$$

where i is the current density, $E(t)$ is the electrode potential, E_{eq} is the equilibrium potential of the reaction (1), α is the anodic transfer coefficient, i_0 is the standard rate constant, $\partial/\partial \mathrm{n}|_\Gamma$ denotes a derivative with respect to the internal normal direction to the surface Γ, F is the Faraday's constant, R is the gas constant, and T is the absolute temperature.

The total current $I(t)$ can be expressed by integrating (8) over the whole surface of the active region of the electrode:

$$I(t) = \iint_{\Gamma_{\mathrm{a}}} i(t)\, \mathrm{d}\Gamma_{\mathrm{a}}. \tag{9}$$

For a single cyclic potential sweep, the electrode potential–time function can be written as

$$E(t) = \begin{cases} E_{\mathrm{eq}} - vt, & \text{for } 0 \leqslant t \leqslant t_{\mathrm{r}}, \\ E_{\mathrm{eq}} - 2vt_{\mathrm{r}} + vt, & \text{for } t > t_{\mathrm{r}}, \end{cases} \tag{10}$$

where v is the sweep rate and t_{r} is the time of reversal of the linear potential–time sweep [11].

3. Digital simulation of experiments

The mathematical model (2)–(8) was used for digital simulation of real experiments. The principal structure of the surface of partially blocked electrodes, used in the experiments, is shown in figure 1(a), where m circular active regions of radius a are arranged in a rigid hexagonal array. Due to the symmetric distribution of the active sites, leaving out of account the resist layer, the diffusion space adjustment to the electrode surface may be divided into m equal hexagonal prisms with regular hexagonal bases. For simplicity, it is reasonable to consider a circle of radius b (figure 1(b)) whose area is equal to that of the hexagon and to regard one of the cylinders as a unit cell of the diffusion space [11]. Due to the symmetry of a cylinder, we may consider only a quarter of the cylinder.

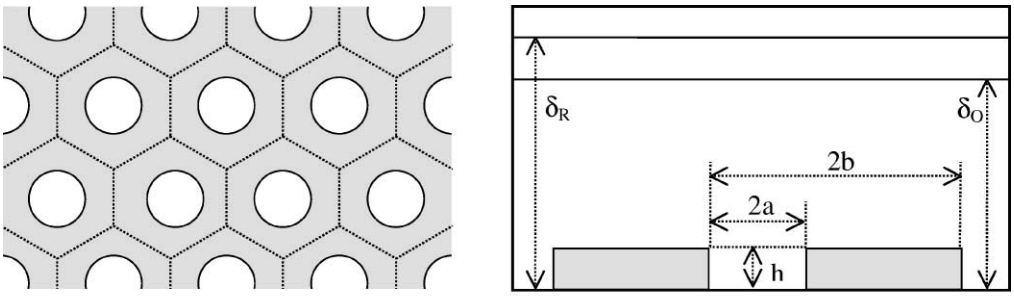

Figure 1. A principal structure of (a) partially blocked electrode and (b) the profile at z plane. Shaded areas indicate the resist layer. The figure is not to-scale.

Now, taking into account the resist layer of thickness h (figure 1(b)), the mathematical model (2)–(8) of the reaction (1) for partially blocked electrodes, shown in figure 1, may be written in cylindrical coordinates (r, z) with

$$\begin{aligned}
&\Gamma_a = \{0 \leqslant r \leqslant a,\ z = 0\},\\
&\Gamma_O^N = \{0 \leqslant r \leqslant b,\ z = \delta_O\}, \qquad \Gamma_R^N = \{0 \leqslant r \leqslant b,\ z = \delta_R\},\\
&\Omega_O = \{0 \leqslant r \leqslant a,\ 0 \leqslant z \leqslant \delta_O\} \cup \{a < r \leqslant b,\ h \leqslant z \leqslant \delta_O\},\\
&\Omega_R = \{0 \leqslant r \leqslant a,\ 0 \leqslant z \leqslant \delta_R\} \cup \{a < r \leqslant b,\ h \leqslant z \leqslant \delta_R\},
\end{aligned} \tag{11}$$

where δ_O and δ_R is the thickness of the Nernst layer for species O and R, respectively.

Some problems arise when analytically solving the differential equations with complex diffusion space and boundary conditions, therefore, the mathematical model represented by (2)–(8) was solved numerically. The finite-difference technique [17] was used for discretization of the model (2)–(8). This technique allows us to solve effectively the differential equations with rather complex diffusion space and boundary conditions.

In the digital simulation, the main problem is an overload of calculation due to the boundary conditions (5)–(7) and permissible conditions: $h \ll \delta_O$, $h \ll \delta_R$, $a \ll b$. Because of the mass transport for both species O and R is independent from each other (see (2) and (3)), and diffusion spaces Ω_O and Ω_R are not identical because of condition $\delta_R \neq \delta_O$, we introduced two non-uniform discrete grids: Δ_O for Ω_O and Δ_R for Ω_R. Because the reaction takes place on the surface of the electrode (on the plane $z = 0$) and the lower surfaces of Ω_O and Ω_R are identical, it was reasonable to use the same discretization of the region of $[0, b] \times [0, h]$.

Because the boundary conditions (6) and (7) are discontinuous at the active/inactive site boundary, to have accurate and stable results it was necessary to use very small step of the grids Δ_O and Δ_R at that boundary in r direction. A constant step of the grids was used in r direction for $r \leqslant a$ (in the active region), while an exponentially increasing step was used for $r > a$ (in the inactive region). Let us notice that it may be reasonable to use an increasing step in r direction from that boundary ($r = a$) to the center of the active site ($r = 0$) as well in modelling of partially blocked electrodes with relatively large active region, for example, with $b/2 < a < b$.

In z direction, we used a non-uniform step as well, due to the condition $h \ll \delta_O$ and $h \ll \delta_R$. A small constant step was used for $z \in [0, h]$. It was assumed that an exponentially increasing step may be used for $z > h$, however, it should not be increased up to the Nernst boundary due to the boundary condition (5). Let l_O and l_R be values from the interval (h, δ_O) and (h, δ_R), respectively, i.e., $l_O \in (h, \delta_O)$, $l_R \in (h, \delta_R)$. An exponentially increasing step was used in segment (h, l_O) in Δ_O and in segment (h, l_R) in Δ_R, while a constant step was kept for greater values of z. Choosing of values of l_O and l_R depends on the degree of step increasing and on the values of δ_O, δ_R, respectively. We employed the following values: $l_O = h + (\delta_O - h)/2$, $l_R = h + (\delta_R - h)/2$.

Let $\bar{t}$ be the time of simulation. The finite difference discretization of (2)–(8) for $\Delta_O \times (0, \bar{t}]$ and $\Delta_R \times (0, \bar{t}]$ was obtained by using a constant step in t direction.

The system of linear equations of implicit finite difference schemes was built as a result of the difference approximation of the problem (2)–(8). The variable direction method [17] was used to decrease the number of independent variables of the system of linear equations. The resulting system of the linear equations was effectively solved due to the tridiagonality of the system.

4. Results of calculation and discussion

Several model electrodes were used in real experiments and numerical simulation of the behavior of the electrodes. Experimental results were published in [18]. The electrodes varied in the blocking degree θ ($\theta = 1 - a^2/b^2$). The area S of the whole surface, including all active and inactive regions, of the every model electrode was 0.48 cm^2. The geometrical data of model electrodes, used in the real experiments, is presented in table 1. We had no possibility to measure precisely the thickness h of the resist layer. The measurement of the resist layer of the model electrodes showed that the thickness was about 1 μm ($h \approx 1$ μm).

The following values of the parameters were constant in numerical simulation of the all experiments:

$$\begin{aligned} &C_{\mathrm{O}}^0 = C_{\mathrm{R}}^0 = 2.5 \times 10^{-5}\ \mathrm{mol/cm^3}, \\ &D_{\mathrm{O}} = 5.8 \times 10^{-6}\mathrm{cm^2/s}, \qquad D_{\mathrm{R}} = 4.8 \times 10^{-6}\ \mathrm{cm^2/s}, \\ &n = 1, \qquad \alpha = 0.5, \qquad T = 293\ \mathrm{K}, \\ &E_{\mathrm{eq}} = 470\ \mathrm{mV}, \qquad E_{\mathrm{r}} = -100\ \mathrm{mV}, \qquad \overline{E} = 900\ \mathrm{mV}, \end{aligned} \tag{12}$$

where E_{r} is the electrode potential at the reversal time t_{r}, i.e., $E_{\mathrm{r}} = E(t_{\mathrm{r}})$ in (10), $\overline{E}$ is the final electrode potential. The value of t_{r} in the numerical simulation of the electrode behavior, was calculated from (10) with a value of E_{r} and a value of the sweep rate v. The electrode potential during the experiments, was decreased (forward or cathodic sweep direction) from E_{eq} to E_{r}, then the electrode potential was increased (reverse or anodic sweep direction) up to $\overline{E}$. There were two sweep rates v: 20 mV/s and 100 mV/s. In all the numerical experiments, values of i_0 in (8) and δ_{O}, δ_{R} in (11) were chosen to have the best fit between the experiments and numerical curves of the current. In addition, the values of i_0 were chosen among values between 0.01 and 0.1 A/cm^2 [10]. An empirical law of $\delta_{\mathrm{O}}\sqrt{v} \approx$ const and $\delta_{\mathrm{R}}\sqrt{v} \approx$ const, which was found to be valid under linear potential sweep condition [19], was used to determine values of δ_{O}, δ_{R}.

Table 1
Geometrical data of model electrodes.

No.	a (μm)	b (μm)	θ
1	23.6	23.6	0
2	10.0	23.6	0.82
3	2.5	23.6	0.989

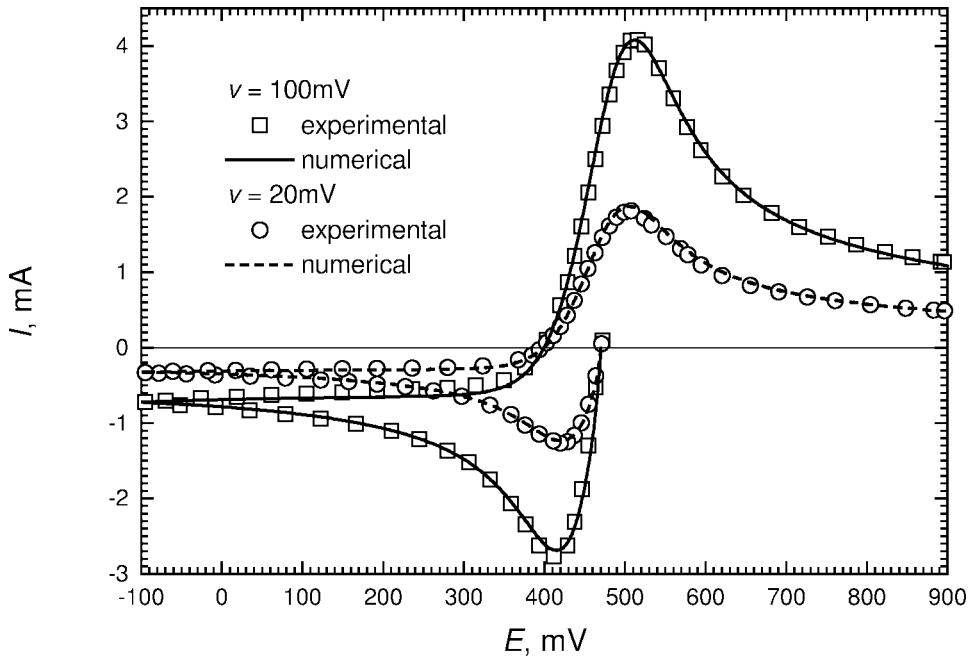

Figure 2. The dynamics of the current for the unblocked electrode No. 1 (table 1) at two sweep rates v: 100 mV/s ($i_0 = 0.015$ A/cm^2, $\delta_O = 110$ μm, $\delta_R = 190$ μm) and 20 mV/s ($i_0 = 0.012$ A/cm^2, $\delta_O = 240$ μm, $\delta_R = 420$ μm). The white squares and circles show experimental data, and the solid and dashed lines are the corresponding numerical solutions at $v = 100$ mV/s and $v = 20$ mV/s, respectively.

The total current $I(t)$ of the model electrodes was measured in the real experiments at various times. In simulation, the current of the unit cell was calculated by numerical integration (8) over the surface of the active region (it is a circle of radius a) of the cell. Then, the current of the unit cell was multiplied by the number m of the unit cells to get the total current of the electrode. Because the area S of the whole surface of the model electrodes was approximately 0.48 cm^2, and the radius b of the unit cell was 23.6 μm, then m was about 27430 ($m = S/(\pi b^2)$).

Firstly, the model was used for numerical simulation of the unblocked electrode (No. 1 in table 1). There are no inactive sites at all in this extreme case of the blocking degree. So, $a = b$, $h = 0$ with $\theta = 0$. The thickness δ_O and δ_R of the Nernst diffusion layer was chosen as $\delta_O = 240$ μm, $\delta_R = 420$ μm at $v = 20$ mV/s and $\delta_O = 110$ μm, $\delta_R = 190$ μm at $v = 100$ mV/s. In numerical solution, accurate and stable results were achieved when the radius a of the active site of the unit cell was divided into 50 increments, and the minimum step in z direction was equal to $\min(\delta_O, \delta_R)/10^3$ (0.24 μm at $v = 20$ mV/s and 0.11 μm at $v = 100$ mV/s). The step in t direction was 10^{-2} s at $v = 20$ mV/s and 2×10^{-3}s at $v = 100$ mV/s. Results of the calculation are depicted in figure 2. As it is possible to notice, the good agreement between the calculated and experimental results is obtained.

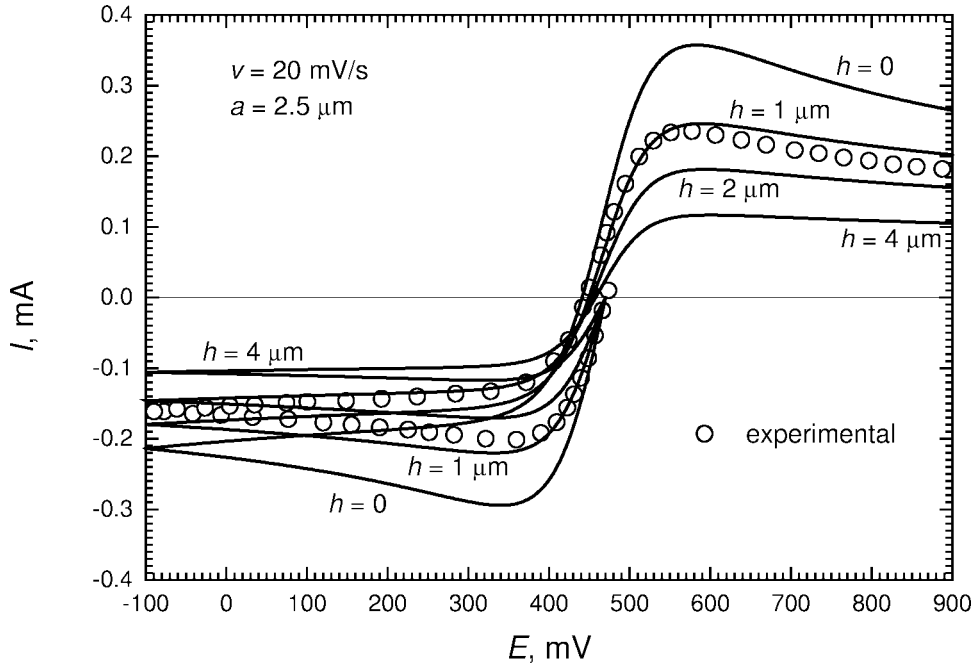

Figure 3. The dynamics of the current for model electrode No. 3 (table 1) at sweep rate $v = 20$ mV/s. h is the thickness of resist layer, where h is from set $\{0, 1, 2, 4\}$ μm, $\delta_O = 280$ μm, $\delta_R = 340$ μm and $i_0 = 0.1$ A/cm^2. The white circles show experimental data, and the solid lines are numerical ones.

Then the electrochemical behavior of several partially blocked electrodes (No. 2 and 3 in table 1) was simulated. At first, we did not take into account the resist layer, following the known assumption [10] that the influence of the thickness of the resist layer of 1–2 μm would be negligible because of the thickness is much smaller than the radius of the unit cell. Results of calculation showed that calculated maximal currents were rather greater (up to 40%) than the experimental maximal currents. Therefore, the resist layer was introduced into the mathematical model (2)–(8), i.e., into the definition of the diffusion space Ω_O and Ω_R (11) of the model (2)–(8).

The thickness δ_O and δ_R of the Nernst diffusion layer in modelling of electrodes No. 2 and 3 (see table 1) was chosen as $\delta_O = 280$ μm, $\delta_R = 340$ μm at potential sweep rate v of 20 mV/s and $\delta_O = 125$ μm, $\delta_R = 150$ μm at $v = 100$ mV/s. Accurate and stable results of numerical simulation were achieved when the radius a of the active site of the unit cell was divided into 200 increments, i.e., the minimum step was 0.05 μm for electrode No. 2 and 0.0125 μm for electrode No. 3, while the minimum step was 0.47 μm in the case of the unblocked electrode No. 1. The minimum step in z direction was used as $\min(\delta_O, \delta_R)/10^4$ (0.028 μm at $v = 20$ mV/s and 0.0125 μm at $v = 100$ mV/s). So, the minimum step of the discrete grid Δ_O and Δ_R in both space directions (r, z) was by the order of magnitude lower than the corresponding minimum step in numerical modelling of the unblocked model eletrode. It can be explained by the discontinuity of the boundary conditions (6) and (7) and relatively small thickness h of the resist layer

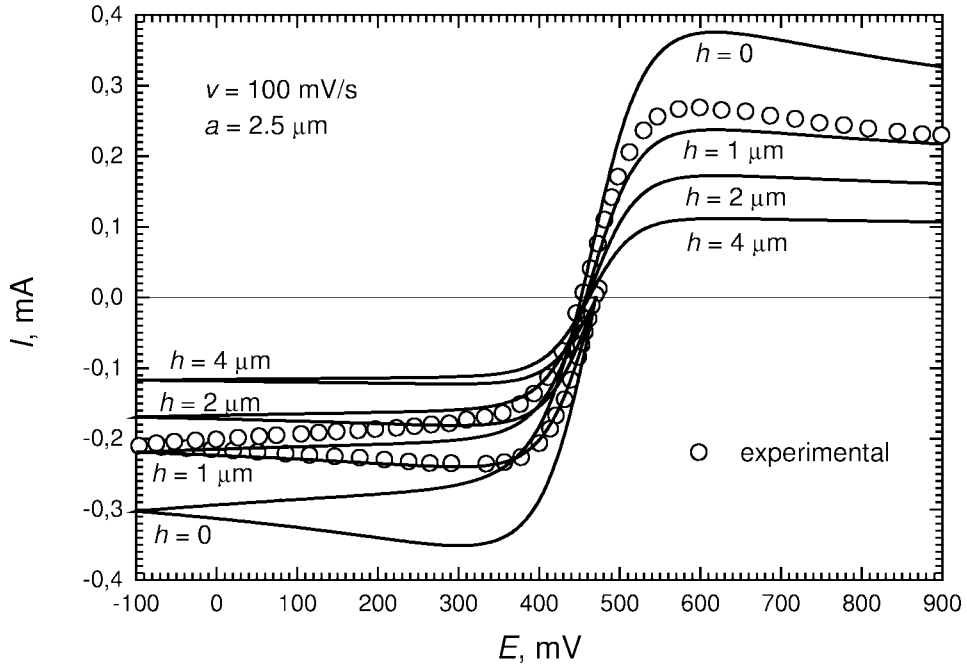

Figure 4. The dynamics of the current for model electrode No. 3 (table 1) at sweep rate $v = 100$ mV/s. The thickness h of the resist layer is from set $\{0, 1, 2, 4\}$ μm. $\delta_O = 125$ μm, $\delta_R = 150$ μm and $i_0 = 0.1$ A/cm^2. The white circles show experimental data, and the solid lines are numerical ones.

(h was from set $\{1, 2, 4\}$ μm), i.e., $h \ll \min(\delta_O, \delta_R)$. The step in t direction was the same as in modelling of the unblocked electrode. In numerical modelling of an extreme case of $h = 0$, the minimum step in z direction was the same as in case of unblocked electrode. Results of the calculation are depicted in figures 3–5.

The influence of the thickness of the resist layer, as seen in figures 3 and 4, appears to be important for highly blocked electrode ($\theta = 0.989$). The good agreement between the calculated and experimental results is obtained at resist layer thickness (h) of about 1 μm. These values of the thickness compare favorably with the values given by experimental measurement of the resist layer of the model electrodes. Figures 3 and 4 show that the cathodic (forward) and anodic (reverse) maximal currents are about 25–40% less for the thickness h of the resist layer of 1 μm in comparison with the case of $h = 0$. This property is valid for both sweep rates: 20 mV/s (figure 3) and 100 mV/s (figure 4).

While comparing figure 3 with figure 5, one can see that the influence of the resist layer on values of the current is less meaningful for an electrode with the less blocking degree at the same sweep rate. In other words, the effect of the resist layer is more enhanced with the increase of the blocking degree.

The investigation of the influence of the resist layer on the behavior of the partially blocked electrodes was generalized. The similar investigation of the influence of the diffusion space geometry on dynamics of the current can be found in [20]. Let $I^c_{h,\theta}$ be the cathodic peak current and $I^a_{h,\theta}$ the anodic one for the model electrode with blocking

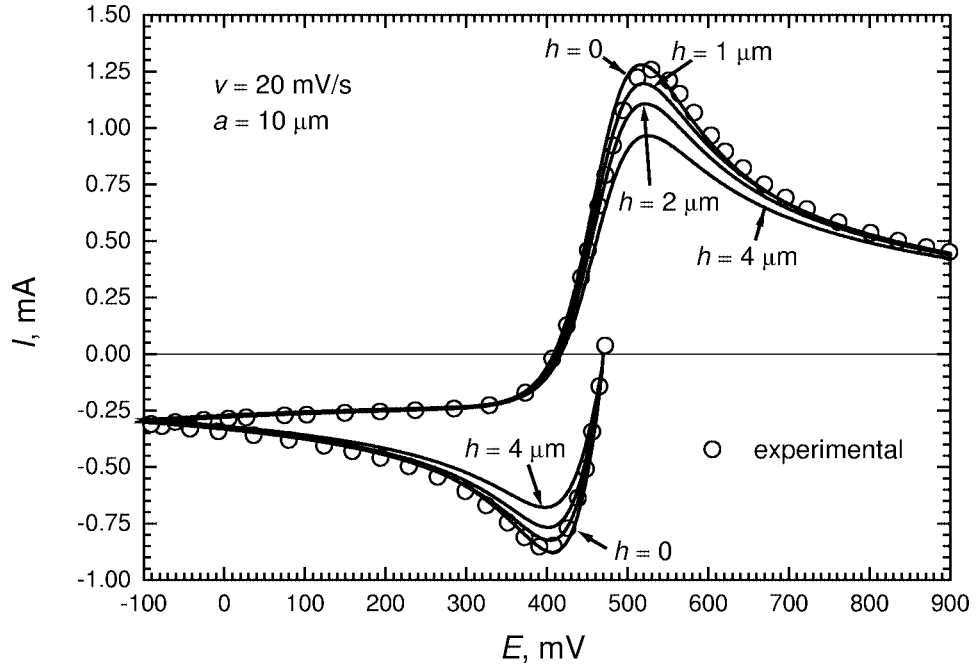

Figure 5. The dynamics of the current for model electrode No. 2 (table 1) at sweep rate $v = 20$ mV/s. Values of δ_O, δ_R, and i_0 are the same as in figure 3. The thickness h of the resist layer is from set {0, 1, 2, 4} μm. The white circles show experimental data, and the solid lines are numerical ones.

degree of θ and the resist layer thickness of h (μm). Values of $I^c_{h,\theta}$ and $I^a_{h,\theta}$ were calculated for various values of the parameter θ ($0 < \theta < 1$) and two values of h: 0 (no resist layer) and 1 μm. Let k_c be a dimensionless ratio of the cathodic peak current $I^c_{1,\theta}$ to $I^c_{0,\theta}$, and k_a a ratio of the anodic peak current $I^a_{1,\theta}$ to $I^a_{0,\theta}$, i.e., $k_c = I^c_{1,\theta}/I^c_{0,\theta}$, $k_a = I^a_{1,\theta}/I^a_{0,\theta}$. Figure 6 shows the variation of the ratio k_c and k_a with blocking degree. In this calculation, values of $v = 100$ mV/s, $\delta_O = 125$ μm, $\delta_R = 150$ μm and $i_0 = 0.05$ A/cm^2 were employed. Curves drawn through all calculated values are functions:

$$(1-\theta)\left(\frac{p_1}{p_2-\theta}+\frac{p_3}{p_4-\theta}+p_5\right), \tag{13}$$

where $p_1 = 0.611$, $p_2 = 1.001$, $p_3 = 0.293$, $p_4 = 1.02$, $p_5 = 0.106$ for k_c and $p_1 = 0.665$, $p_2 = 1.001$, $p_3 = 0.39$, $p_4 = 1.03$, $p_5 = -0.04$ for k_a. A significant decrease in k_c as well as k_a with the increase in the blocking degree can be seen in figure 6. Note the $k_c \approx k_a \approx 1$, i.e., $I^c_{1,\theta} \approx I^c_{0,\theta}$ and $I^a_{1,\theta} \approx I^a_{0,\theta}$ when blocking degree θ becomes about 0. Values of k_c and k_a notably decrease for higher values of the blocking degree θ ($\theta > \approx 0.8$). So, the resist layer of thickness of 1 μm appears to be important for the peak currents, and it is especially important for highly blocked electrodes. Particularly, the cathodic peak current is more sensitive to the resist layer than the anodic one. Additional calculation showed the similar variation of k_c and k_a with blocking degree at the sweep rate of $v = 20$ mV/s.

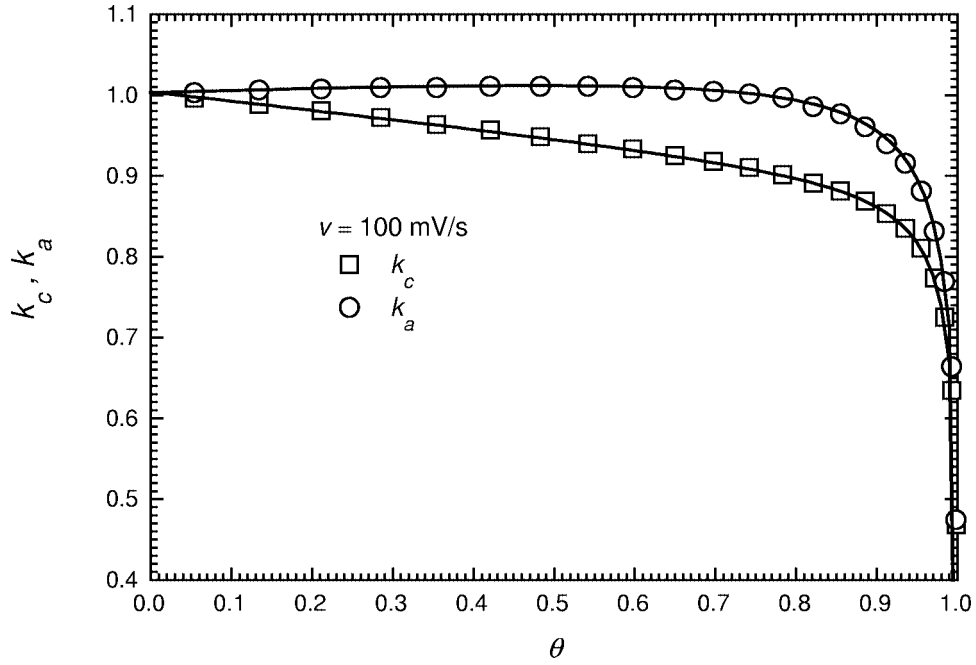

Figure 6. The dependence of the normalized cathodic (k_c) and anodic (k_a) peak current on the blocking degree θ at sweep rate $v = 100$ mV/s. Values of δ_O and δ_R are the same as in figure 4, $i_0 = 0.05$ A/cm^2. The white rectangles and circles show calculated values of k_c and k_a, respectively. The solid lines are the corresponding functions (13) fitted to these values.

5. Conclusions

The mathematical model (2)–(8) may be used successfully for the simulation of electrochemical behavior of partially blocked as well as unblocked electrodes. The mass transport may be assumed to be regular in the entire diffusion space. In simulation of behavior of the partially blocked electrodes, the resist layer of thickness of 1 μm should be taken into account to obtain the good agreement between experimental and numerical results for highly blocked electrodes ($\theta > \approx 0.8$). The thickness of the resist layer is a parameter of the model, which can be measured experimentally. The influence of the resist layer on the cathodic and anodic peak current increases with the blocking degree.

References

[1] K. Aoki, Electroanalysis 5 (1993) 627.
[2] B.R. Scharifker, J. Electroanalyt. Chem. 240 (1988) 61.
[3] C. Lee, C.J. Miller and A.J. Bard, Analyt. Chem. 63 (1991) 78.
[4] H. Reller, E. Kirowa-Eisner and E. Gileadi, J. Electroanalyt. Chem. 138 (1982) 65.
[5] H. Reller, E. Kirowa-Eisner and E. Gileadi, J. Electroanalyt. Chem. 161 (1984) 247.
[6] R.M. Wightamm and D.O. Wipf, in: *Electroanalytical Chemistry*, Vol. 15, ed. A.J. Bard (M. Dekker, New York, 1989) pp. 267–353.

[7] P. de Oliveira, L. Jiang, S. Kaneko, A. Aitken, P.A. Leigh, P.J. Dobson and H.A.O. Hill, in: *45th Annual ISE Meeting*, Porto (1994) OVI-4.
[8] B.R. Horrocs, M.V. Mirkin, D.T. Pierce, A.J. Bard, G. Nagy and K. Toth, Analyt. Chem. 65 (1993) 1213.
[9] K. Aoki, M. Morita, O. Niwa and H. Tabei, J. Electroanalyt. Chem. 256 (1988) 269.
[10] T. Gueshi, K. Tokuda and H. Matsuda, J. Electroanalyt. Chem. 89 (1978) 247.
[11] T. Gueshi, K. Tokuda and H. Matsuda, J. Electroanalyt. Chem. 101 (1979) 29.
[12] K. Tokuda, T. Gueshi and H. Matsuda, J. Electroanalyt. Chem. 102 (1979) 41.
[13] C. Deslous, C. Gabrielli, M. Keddam, A. Khalil, R. Rosset, B. Trobollet and M. Zidoune, Electrochim. Acta 42 (1997) 1219.
[14] J. Hitzig, J. Titz, K. Juttner, W.J. Lorenz and E. Schmidt, Electrochim. Acta 29 (1984) 287.
[15] E. Schmidt, J. Hitzig, J. Titz, K. Juttner and W.J. Lorenz, Electrochim. Acta 31 (1986) 1041.
[16] A.J. Bard, Analyt. Chem. 33 (1961) 11.
[17] A.A. Samarskii, *The Theory of Difference Schemes* (Nauka, Moscow, 1989) (in Russian).
[18] A. Survila, P.V. Stasiukaitis, S. Kanapeckaitė and V. Uksienė, Chemija (Vilnius) 2 (1998) 143.
[19] A. Survila, P.V. Stasiukaitis and S. Kanapeckaitė, Chemija (Vilnius) 2 (1998) 138.
[20] R. Baronas, F. Ivanauskas and J. Kulys, J. Math. Chem. 25 (1999) 245.